An Efficient Numerical Scheme for Evaluating the Rolling Resistance of a Pneumatic Tire

H.Golbakhshi [1], M.Namjoo [2]

1, 2 Instructor, Department of Mechanical Engineering and Department of Mechanical Engineering of Bio systems, University of Jiroft, 78671-61167, Jiroft, Iran.

Abstract

The viscoelastic effect of rubber material on creation of rolling resistance is responsible for 10-33% dissipation of supplied power at the tire/road interaction surface. So, evaluating this kind of loss is very essential in any analysis concerned with energy saving. The transient dynamic analysis for including the rolling effects of the tire requires long CPU time and the obtained results are prone to considerable numerical oscillations. By adding the equivalent loads to static interaction of tire with the road, an efficient 3D FE analysis is presented for evaluating the dissipated energy of a rolling tire. The results closely match the related experimental and numerical investigations.

Keywords*: FE method, numerical simulation, hysteresis loss, rolling resistance, strain energy.*

1. Introduction

In recent years, reducing the fuel consumption has become increasingly important issue for both governments and car manufacturers. Despite the aerodynamic drag and losses concerned with engine and powertrain systems, the rolling resistance at tire/road interaction surface is responsible for 10-33% dissipation of supplied power depending on tire structure and amount of axle load. So, developing efficient tires plays a crucial role for improving the fuel consumption of vehicles [1-3]. Due to viscoelastic hysteresis property of rubber components, the cyclic deformations of rolling tire contribute to tire rolling resistance [4, 5]. So, evaluation of hysteretic loss is very essential in any analysis concerned with fuel economy of automobiles and energy conservation. Experimental measurements for rolling resistance clearly indicate the complex relationship between influential parameters and operating conditions [6]. However, experimental investigations are costly and time consuming.

In recent decades, using finite element analysis as a viable method, a lot of investigations have been performed on design of efficient tires [7-9]. All the numerical methods used for the analysis of pneumatic tires have in common the fact that the time histories of strains must be approximated to calculate the hysteretic loss and rolling resistance [2]. In early works, sector- wise Fourier series were used for approximation of strain cycles [10, 11]. Later, using the transient dynamic analysis for rolling, more realistic results were obtained for the strain cycles and hysteretic loss [12-16]. However, including the rolling effect in simulation requires long CPU time; furthermore the obtained results for strains have a considerable oscillation which affects the accuracy of the analysis.

In this study, without considering the rolling motion, an efficient 3D FEM model of tire/road interaction is prepared for evaluating hysteretic loss and resulting rolling resistance created inside the tire body. Compared with investigations based on dynamic rolling analysis, the results of proposed method for rolling resistance have a considerable consistency and accuracy.

2. Tire construction

Today, common radial tires used in vehicles are made as composite layers of different materials such as nylon, steel cable and rubber. So, two main categories of components can be found for a pneumatic tire structure: 1) the carcass and wear resistant blocks of tread, as two main rubber parts, withstand internal-external loads and provide necessary traction at leading and trailing edges of tire, respectively. 2) Several layers of circumferential belts which are laid to stiffen the treads and strengthen the carcass or the tire body and preventing excessive deformation of the rubber (Fig. 1).

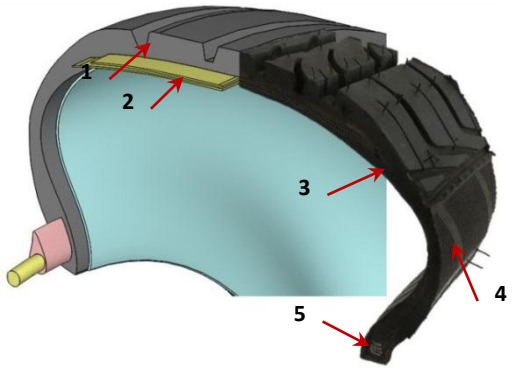

1- Tread

2- Steel belt layers

3- Carcass

4- Sidewall

5- Bead.

Fig1. Structure of a common radial-ply tire 185/60R15 (Right) and 3D model of tire constructed according to the actual size of radial tire in Solid works Simulation (Left).

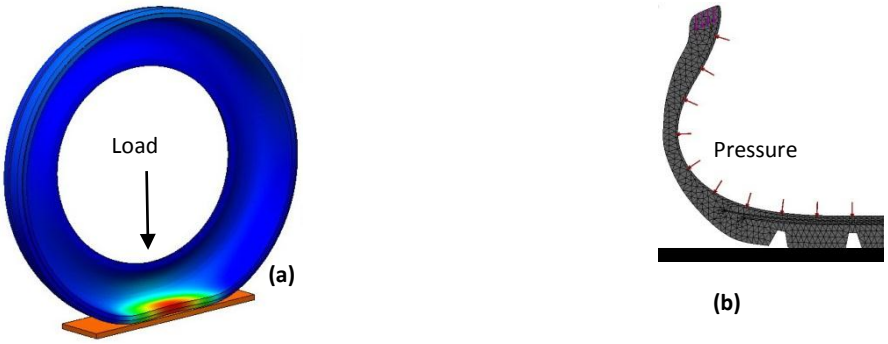

Fig2. Figure 2. Imposition of boundary conditions: (a) 3-D model of the tire/road contact and (b) Cross section of model for inserting inflation pressure on tire inner surface

3. Materials and methods

Due to viscoelastic behavior of rubber compounds, cyclic deformations and oscillating strains resulting from rolling a tire leads to dissipation of mechanical energy and hysteretic loss [11]. Dividing the hysteretic loss by the travelling distance during one revolution, the rolling resistance of the tire can be obtained from the following equation:

$$RR = \frac{W_{loss}}{2\pi\rho_{rr}} \quad (1)$$

Where RR is the rolling resistance and ρ_{rr} is valid rolling radius of the tire.

According to the experimental analysis made by Lin and Hwang, about 10% of tire provided energy is dissipated which is regarded as the main source for rolling resistance [17, 18]. So, in any related numerical prediction the main issue is the evaluation of total stored energy within the tire body. The total stored energy W_{tot} is given by the following generalized form equation:

$$W_{tot} = \int_{\forall}\int_{0}^{t_c} \sigma_{ij}(t)\frac{d\varepsilon_{ij}(t)}{dt}dt\,d\forall \quad (2)$$

Where $\forall$ is the tire volume, t_c is frequency of tire rotation and σ_{ij} and ε_{ij} are components of stress and strain tensors. Based on non-linear Mooney-Rivlin material model, local stresses and strains within domain of an inflated and loaded tire, needed for evaluating the stored strain energy, are related by the following formulation [19, 20].

$$\sigma = 2\left(\lambda - \frac{1}{\lambda^2}\right)\left(C_{01} + \frac{C_{10}}{\lambda}\right) \quad (3)$$

Where, σ is the stress, $\lambda = 1+\varepsilon$ is the extension ratio and ε is the strain. C01 and C10 are the Mooney-Rivlin constants which can be experimentally determined for a variety of working temperatures [21]. The static contact of pneumatic tire with rigid and terrain surfaces are successfully investigated by many authors [2, 20-22]. However, by including a distributed centrifugal load to the tire/road interaction analysis, the rolling motion of tire can be efficiently modeled for evaluating the total stored strain energy and rolling resistance.

4. Results and discussions

In this work, using Solidworks Premium a detailed 3D model of 185/60R15 steel belted radial tire is prepared for calculating the viscoelastic loss and rolling resistance. As shown in Fig. 1 the carcass ply, rubber and steel belts, bead region and tread layer are considered for the tire. The material properties of base rubber and reinforcement parts and other parameters are given in Table 1. It is noted that the mechanical behavior of the rubber varies as the temperature changes. However, in this study the effect of tire temperature is ignored. Because of symmetry in geometry, loading and boundary conditions just half of tire body is modeled for reducing the computing cost and CPU time of the problem (Fig 2.) The total number of 33565 elements and 60661 nodes are used for the entire FEM meshes where all solid triangular element types with 16 jacobian points are chosen from COSMOS. For improving the accuracy of the simulation, finer meshes are used in tire/road contact area.

In order to impose the boundary conditions of the problem, the inflation pressure is applied on internal surfaces of the tire model. Then, the inflated tire is pushed on the rigid surface of road by the axle load (Fig. 2).

The proper contact conditions are applied to the nodes which are located on interacting surface of the tire. In the bead region, all the nodes in contact with the rim are considered to be fixed. The coefficient of friction between the tire and the rigid surface is set to be 0.9. Such high value for friction coefficient guarantees the no- slip condition for the tire motion and all the resistance against motion would be due to the hysteresis loss.

.

Table 1. Material properties used in tire FE model [23].

	Tread	Belt	Carcass	Air
Mooney-Rivlin constants (Mpa)				
C_{01}	2.0477	-	-	-
C_{10}	1.1859	-	-	-
Density, ρ $\left(kg/m^3\right)$	1140	7644	1390	-
Modulus of elasticity, E (Gpa)		55	0.794	-
Poisson ratio, υ		0.3	0.45	-
Hysteresis constant, H	0.1	-	-	-

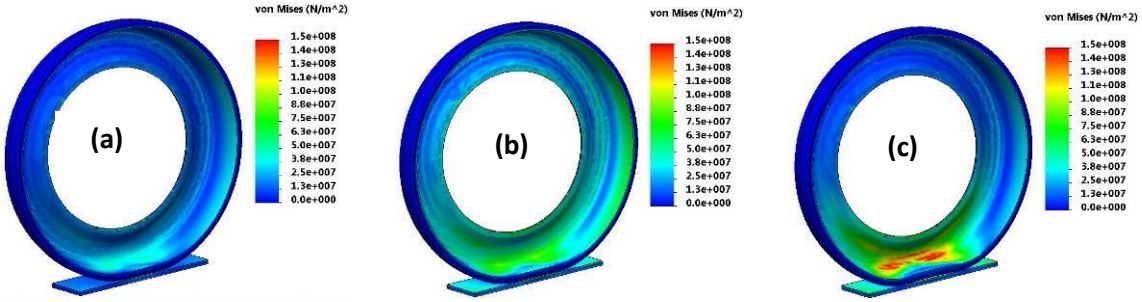

Fig3. Variations of maximum Von-mises stress for $200\,kPa$ inflation pressures and three axel loads: a) $F=3kN$, b) $F=4kN$ and c) $F=5kN$.

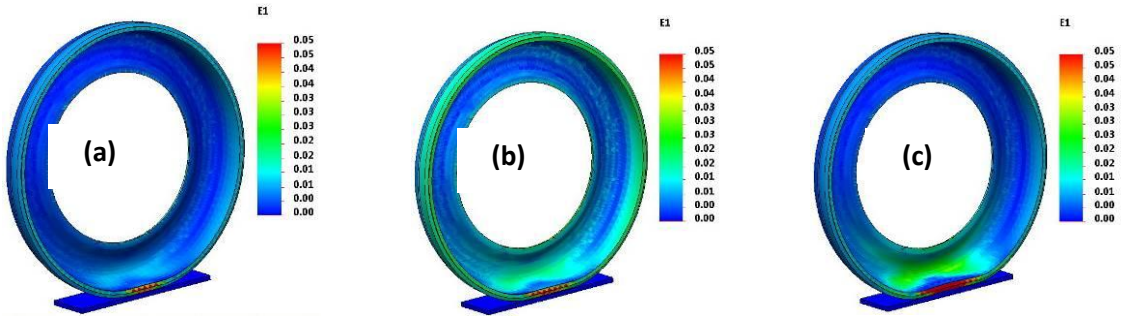

Fig4.. Overall distribution of the maximum principal strain for $200\ kPa$ inflation pressure and three axel loads: a) $F = 3kN$, b) $F = 4kN$ and c) $F = 5kN$

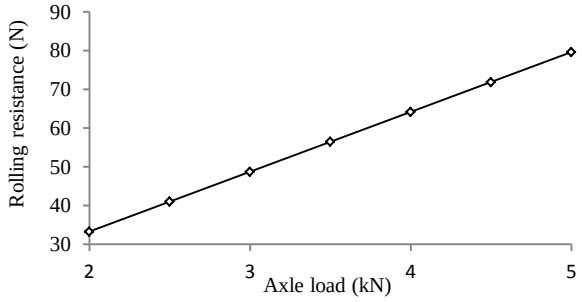

Fig5. Variation of rolling resistance with axle load.

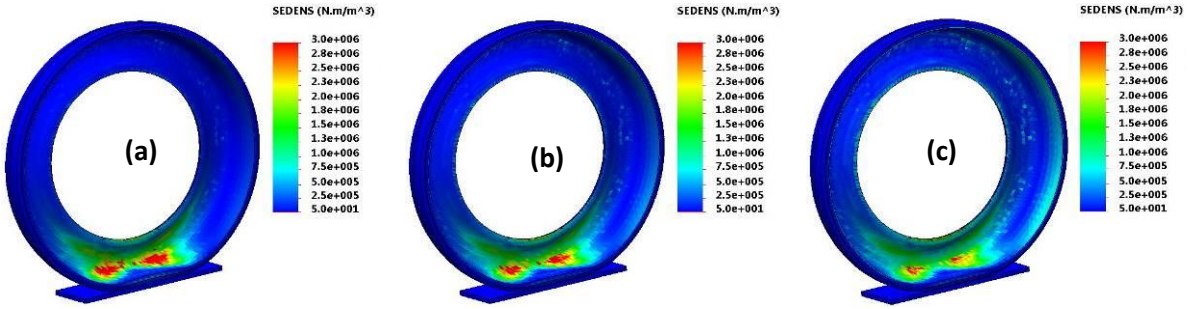

Fig6. Contour plots of strain energy density of a steady-state rolling tire generated by $F = 5\ kN$ for three inflation pressure: (a) $P = 200\ \ kPa$; (b) $P = 300\ kPa$ and (c) $P = 400\ \ kPa$

For different values of axle loads and inflation pressure, the results for gradients of stress and strains are depicted in Figs. 3 and 4. It can be noted that for the same inflation pressure of $200\ kPa$, more severe stress and strain gradients are created by increasing axle loads. As shown in Fig. 3, the maximum value of Von-mises stress is occurred on the contact region of tire with the road. While, the maximum amount of principal strains are located on the tire sidewalls. The obtained results are in a good agreement with available published works [24-27]. As mentioned earlier, by evaluating the stresses and strains caused by external loading, the strain energy stored within the tire body and the amount of rolling resistance can be readily estimated. For variety of inflation pressures and ambient temperatures, the gradients of strain energy density are illustrated in Figs. 6 and 8.

In each case, the high strain values are observed in the vicinity of contact region. Variation of rolling resistance with the axle load is shown in Fig. 5. As the inserted load increases, the amount of dissipated energy will increase and the effective radius of rolling tire will reduce. So, as it can be seen, any increase in axle load leads to double increase in rolling resistance. This trend is fully consistent with the results of related experimental studies [28-30]

It is evident from the results that hysteretic loss lowers as inflation pressure of rolling tire increases.

Variation of rolling resistance with inflation pressure can be observed in Fig. 7. It can be noted that by increasing the pressure from 200 to 400 kPa, an almost value of 32% decrease in a rolling resistance will occur which is similar to that observed in the published results.

Variation of rolling resistance with ambient temperature is shown in Fig. 9. It can be easily found that as the ambient temperature varies from 20 to 40 $^{\circ}C$, the rolling resistance will be reduced by 9.5 %. This reduction is directly related to the reduction of hysteretic loss in higher temperature.

Similar to the published experimental results [28, 30-32], it can be noted from Fig. 10 that the rolling resistance is approximately constant with increasing in speed. However, a slight reduction is noticed from 40-60 km/hr which is regarded as results of higher energy losses at speeds up to 40 km/hr .This behavior closely match the trend of experimental observations.

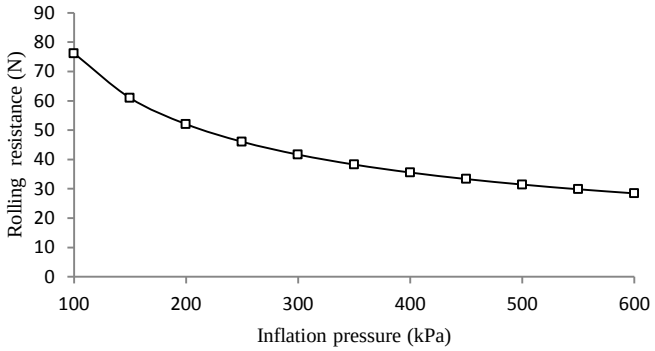

Fig7. Variation of rolling resistance with inflation pressure

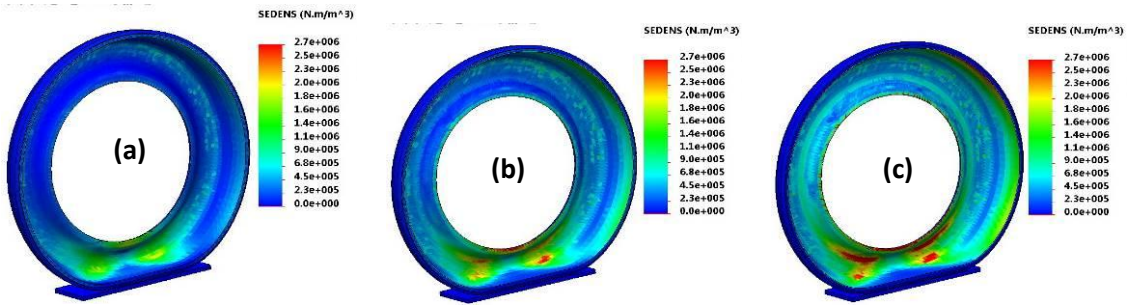

Fig8. Contour plots of strain energy density of a steady-state rolling tire generated by $P = 200$ kPa, $F = 5$ kN for three ambient temperatures: (a) $-10^{\circ}C$ (winter); (b) $15^{\circ}C$ (spring) and (c) $40^{\circ}C$ (summer)

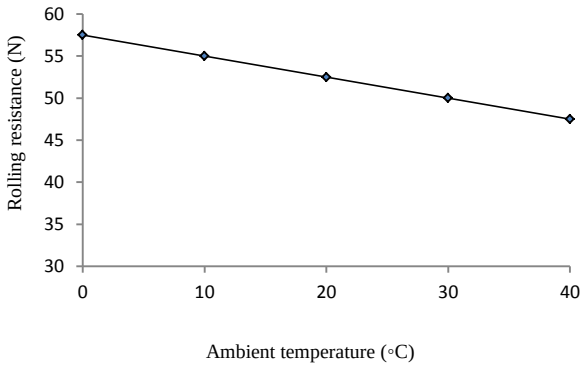

Fig9. Variation of rolling resistance with inflation pressure

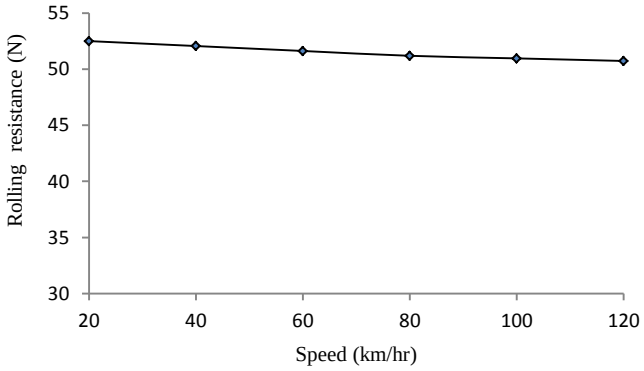

Fig10. Variation of rolling resistance with speed.

5. Conclusion

In this study an efficient numerical scheme is presented for evaluating the impact of different working conditions on dynamic effects and rolling resistance of a moving tire. It is found from the results that the rolling resistance seems to be constant with the increase in speed. Relation between rolling resistance and the axle load is approximately linear. So, a coefficient can be defined for selecting the most suitable wheel load for the tire. Rolling resistance increases with decrease of inflation pressure. It can be concluded that the increased deformations result in a larger rolling resistance. Furthermore, for an $1^{o}C$ increase in ambient temperature, an approximate drop of 0.25 % is noted for rolling resistance. In each case, the obtained results have considerable consistency with related published works.

. Reference

[1]. V. Hublau, and A. Barillier, The Equations of the Rolling Resistance of a Tire Rolling on a Drum, Tire Science and Technology, 36 (2) (2008) 146-155

[2]. J. R. Cho, H. W. Lee, W. B. Jeong, K. M. Jeong, and K. W. Kim, Numerical estimation of rolling resistance and temperature distribution of 3-D periodic patterned tire, International Journal of Solids and Structures, 50 (1) (2013) 86-96

[3]. H. Bettaieb, Improvement of the railway vehicle performance in circulation in curve, Mechanics & Industry, 9 (04) (2008) 335-346

[4]. H. B. Pacejka, Tyre and vehicle dynamics, 2002, Butterworth-Heinemann, ISBN 0, 7506 (5141) (2006) 5

[5]. A. Zouaghi, M. Chafra, and Y. Chevalier, Modeling of composite multilayer rubber-steel: vibro-acoustic insulation of vehicle brake system, Mechanics & Industry, 13 (03) (2012) 185-195

[6]. J. Y. Wong, Theory of ground vehicles, Wiley. com, 2001

[7]. M. Asad, T. Mabrouki, H. Ijaz, M. Aurangzeb Khan, and W. Saleem, On the turning modeling and simulation: 2D and 3D FEM approaches, Mechanics & Industry, FirstView (2014) null-null

[8]. P. Burry, H. Maitournam, and G. Billotey, Éléments-finis étendus pour la modélisation des structures soudées par points, Mechanics & Industry, 9 (02) (2008) 103-108

[9]. H. Golbakhshi, M. Namjoo, and M. Mohammadi, A 3D comprehensive finite element based simulation for best Shrink Fit design process, Mechanics & Industry, 14 (01) (2013) 23-30
[10]. J. Mc Allen, A. Cuitino, and V. Sernas, Numerical investigation of the deformation characteristics and heat generation in pneumatic aircraft tires: Part II. Thermal modeling, Finite elements in analysis and design, 23 (2) (1996) 265-290
[11]. T. Ebbott, R. Hohman, J.-P. Jeusette, and V. Kerchman, Tire temperature and rolling resistance prediction with finite element analysis, Tire Science and Technology, 27 (1) (1999) 2-21
[12]. J. Cho, K. Kim, W. Yoo, and S. Hong, Mesh generation considering detailed tread blocks for reliable 3D tire analysis, Advances in engineering software, 35 (2) (2004) 105-113
[13]. J. Cho, K. Kim, and H. Jeong, Numerical investigation of tire standing wave using 3-D patterned tire model, Journal of sound and vibration, 305 (4) (2007) 795-807
[14]. J. R. Luchini, and J. A. Popio, Modeling Transient Rolling Resistance of Tires 3, Tire Science and Technology, 35 (2) (2007) 118-140
[15]. J. Qi, J. Herron, K. Sansalone, W. Mars, Z. Du, M. Snyman, and H. Surendranath, Validation of a Steady-State Transport Analysis for Rolling Treaded Tires 5, Tire Science and Technology, 35 (3) (2007) 183-208
[16]. E. Esmailzadeh, G. Nakhaie-Jazar, and B. Mehri, vibration of road vehicles with non linear suspensions, International Journal of Engineering, 10 (4) 209
[17]. P. S. Pillai, Efect of tyre overload and inflation preasure on olling loss (resistance) and fuel consumption of automobile and truck/bus tires, Indian Journal of Engineering & Materaial Science, 11 (2004) 406-412
[18]. Y.-J. Lin, and S.-J. Hwang, Temperature prediction of rolling tires by computer simulation, Mathematics and Computers in Simulation, 67 (3) (2004) 235-249
[19]. M. H. R. Ghoreishy, A state of the art review of the finite element modelling of rolling tyres, Iranian Polymer Journal, 17 (8) (2008) 571-597
[20]. N. Korunović, M. Trajanović, and M. Stojković, Finite element model for steady-state rolling tire analysis, Journal of the Serbian Society for Computational Mechanics/Vol, 1 (1) (2007) 63-79
[21]. A. Kongo Kondé, I. Rosu, F. Lebon, O. Brardo, and B. Devésa, On the modeling of aircraft tire, Aerospace Science and Technology, 27 (1) (2013) 67-75
[22]. M. Zamzamzadeh, and M. Negarestani, A 3D Tire/Road Interaction Simulation by a Developed Model (ABAQUS Code), Asian Simulation and Modeling, Chiang Mai, Thailand (2007)
[23]. Y. Li, W. Y. Liu, and S. Frimpong, Effect of ambient temperature on stress, deformation and temperature of dump truck tire, Engineering Failure Analysis, 23 (0) (2012) 55-62
[24]. N. Moslem, and G. Hossein, Numerical simulation of tire/soil interaction using a verified 3D finite element model, Journal of Central South University, 21 (2) (2014) 817-821
[25]. R. Moisescu, and G. Frățilă, finite element model of radial truck tyre for analysis of tyre-road contact stress, Scientific Bulletin of University Politehnica of Bucharest, series D (3) (2011) 3-16
[26]. R. E. Smith, T. Tang, D. Johnson, E. Ledbury, T. Goddette, and S. D. Felicelli (2012). "Simulation of Thermal Signature of Tires and Tracks." DTIC Document.
[27]. W. Hall, J. Mottram, and R. Jones, Tire modeling methodology with the explicit finite element code LS-DYNA, Tire science and Technology, 32 (4) (2004) 236-261
[28]. D. Whicker, A. L. Browne, and D. J. Segalman (1981). "Structure and use of GMR combined thermo-mechanical tire power loss model." Society of Automotive Engineers, Inc., Warrendale, PA.